Electronic Supplementary Material (ESI) for Dalton Transactions.

Supporting Information

Lithium, Sodium and Potassium Enolates Aggregates and Monomers: Syntheses and Structures

Nathan Davison, Jack M. Hemingway *, Paul G. Waddell, Erli Lu (陆 而立)*

Chemistry-School of Natural and Environmental Sciences, Newcastle University.

Newcastle upon Tyne, UK. NE1 7RU

Emails: erli.lu@newcastle.ac.uk (E. L.); jack.hemingway@newcastle.ac.uk (J. M. H.)

Contents

1. **General procedures**

All manipulations were carried out using Schlenk techniques, or in a Vigor glovebox equipped with a -35 ^{o}C freezer and a cold well, under an atmosphere of dry argon with the O_2 and H_2O levels <0.5 ppm. Solvents were dried by sodium metal and sodium/potassium alloy, then distilled under vacuum. All solvents were stored in the glovebox over potassium mirrors except for ethers, which were stored over activated 4 Å molecular sieves. The deuterated solvents (d_6-benzene) was distilled from sodium/potassium alloy or activated 4 Å molecular sieves, degassed by three freeze-pump-thaw cycles and stored under argon. **2**-Li [1], **2**-Na [2], **2**-K [3], **4**-Li [4], **4**-Na [2d] and **5**-K [5] are prepared according to the literature protocols. All other chemicals were purchased from Merck, Alfa Aesar and Strem, and dried under dynamic vacuum for 12 hours and stored in the glovebox prior to use.

^{1}H and ^{7}Li NMR spectra were recorded on a Bruker 300 Avance III spectrometer operating at 300.13 and 116.64 MHz respectively. Chemical shifts are quoted in ppm and are relative to $SiMe_4$ (^{1}H) or external 0.1M LiCl in D_2O (^{7}Li). Due to poor solubility of the crystallised products and to ensure consistency, NMR spectra shown are taken from the *in situ* NMR scale reactions, except for the ^{13}C NMR of the monomeric complexes. The complexes **3**-Li/Na/K crystallise out from the NMR scale reaction in short time and can not be re-dissolved, hence their ^{13}C NMR spectra are not avilable. Due to poor solubility of the aggregate complexes in C_6D_6 meaningful ^{13}C NMR spectra were unable to be collected for these complexes.

2. Synthesis and Characterisation of Complexes 3-Li/Na/K & 6-Li/Na

Synthesis of 3-Li ($LiCH_2SiMe_3$ + 9-acetylanthracene)

NMR scale reaction
$LiCH_2SiMe_3$ (0.0028 g, 0.03 mmol) was dissolved in C_6D_6 (0.5 ml). The solution was added to 9-acetylanthracene (0.0066 g, 0.03 mmol) in a one-portion manner. The resulting pale yellow solution was transferred to a J Young NMR tube. NMR was ran 15 minutes after mixing which showed complete reaction to the enolate. Yellow crystals suitable for SCXRD resulted in the NMR tube.

Scale-up:
$LiCH_2SiMe_3$ (0.0942 g, 1 mmol) was dissolved in benzene (1 ml). The solution was added to a solution of 9-acetylanthracene (0.2203 g, 1 mmol) in benzene (1 ml), in a one-portion manner and mixed using a pipette. Complete dissolving resulted to form a yellow solution and after 30 seconds a yellow crystalline solid precipitated out. The mixture was left at room temperature for 1 hour before the mother liquor was removed and the resulting pale yellow solid was dried *in vacuo* (0.2191 g, 97 % yield).

^{1}H NMR (d_6-benzene, 25 ˚C, 300 MHz): δ (ppm) 8.05 (s, 1H), 7.83 – 7.66 (m, 4H), 7.22 – 7.11 (signals overlapping with C_6D_6 signal, m, 2H), 7.04 – 6.92 (m, 2H), 3.64 (d, J = 1.0 Hz, 1H), 3.26 (d, J = 1.0 Hz, 1H).
^{7}Li NMR (d_6-benzene, 25 ˚C, 117 MHz): δ (ppm) 0.50

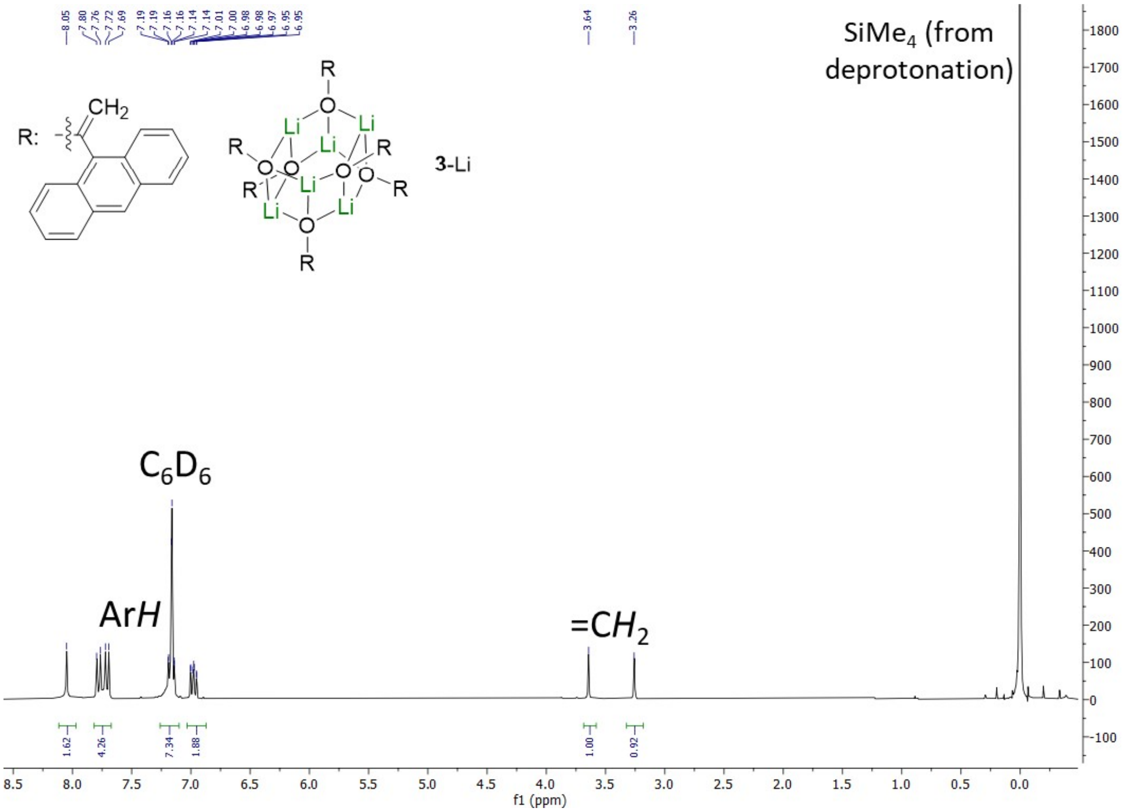

Figure S1: ^{1}H NMR spectrum of an NMR scale reaction between $LiCH_2SiMe_3$ and 9-acetylanthracene to form **3-Li** and $SiMe_4$ in C_6D_6 at 298 K.

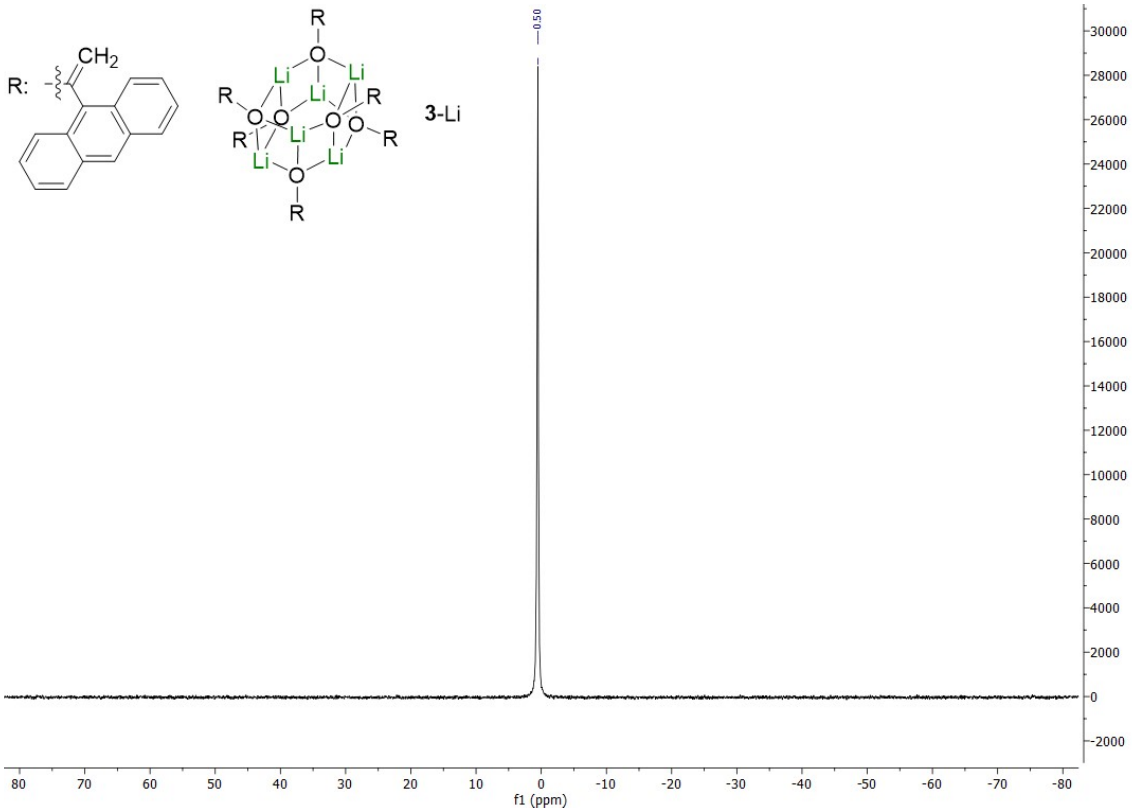

Figure S2: ^{7}Li NMR spectrum of an NMR scale reaction between $LiCH_2SiMe_3$ and 9-acetylanthracene to form **3-Li** and $SiMe_4$ in C_6D_6 at 298 K.

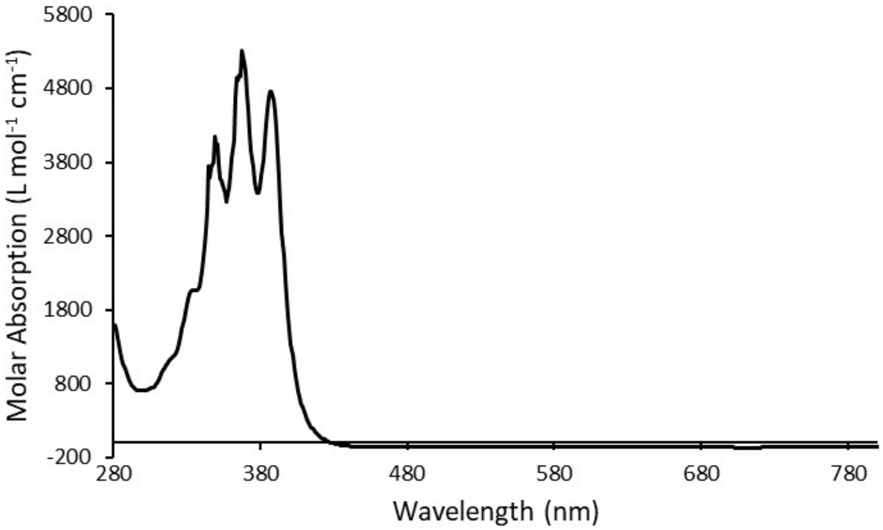

Figure S3: UV/Vis spectrum of **3-Li**. The data was collected on a 0.5 mM benzene solution at 298 K.

Synthesis of 6-Li ([Li(CH_2SiMe_3)(Me_6Tren)] + 9-acetylanthracene)

NMR scale reaction:

[Li(CH_2SiMe_3)(Me_6Tren)] (0.0097 g, 0.03 mmol) was dissolved in C_6D_6 (0.5 ml). The solution was added to 9-acetylanthracene (0.0066 g, 0.03 mmol) in a one-portion manner. The resulting orange solution was transferred to a J Young NMR tube. NMR was ran 15 minutes after mixing which showed complete reaction to the enolate.

Scale-up:
[LiCH_2SiMe_3)(Me_6Tren)] (0.1623 g, 0.5 mmol) was dissolved in benzene (1 ml). The solution was added to a solution of 9-acetylanthracene (0.1101 g, 0.5 mmol) in benzene (1 ml), in a one-portion manner. The resulting orange solution was left at room temperature for 15 minutes, before the volatiles were removed *in vacuo*. An orange solid resulted. The solid was dissolved in a mixture of hexane (4 ml) and toluene (7 ml). The resulting solution was filtered and placed in a -35 °C freezer. Orange crystals suitable for SCXRD resulted overnight. The mother liquor was removed and the crystals were dried *in vacuo* (0.1826 g, 80 % yield).

^{1}H NMR (d_6-benzene, 25 ˚C, 300 MHz): δ (ppm) 9.35 (d, J = 8.8 Hz, 2H), 8.17 (s, 1H), 7.94 – 7.84 (m, 2H), 7.49 – 7.27 (m, 4H), 4.75 (d, J = 2.0 Hz, 1H), 4.27 (d, J = 2.0 Hz, 1H), 1.88 (s, br, 18H), 1.77 (s, br, 12H)
^{13}C NMR: (d_6-benzene, 25 ˚C, 75 MHz): δ (ppm) 132.6 (quaternary Ar*C*), 130.0, 127.7, 124.5, 122.8 (Ar*C*H), 79.4 (=*C*H_2), 56.5 (Me_6Tren-*C*H_2), 50.4 (Me_6Tren-*C*H_2), 45.0 (Me_6Tren-*C*H_3).
^{7}Li NMR (d_6-benzene, 25 ˚C, 117 MHz): δ (ppm) 0.28

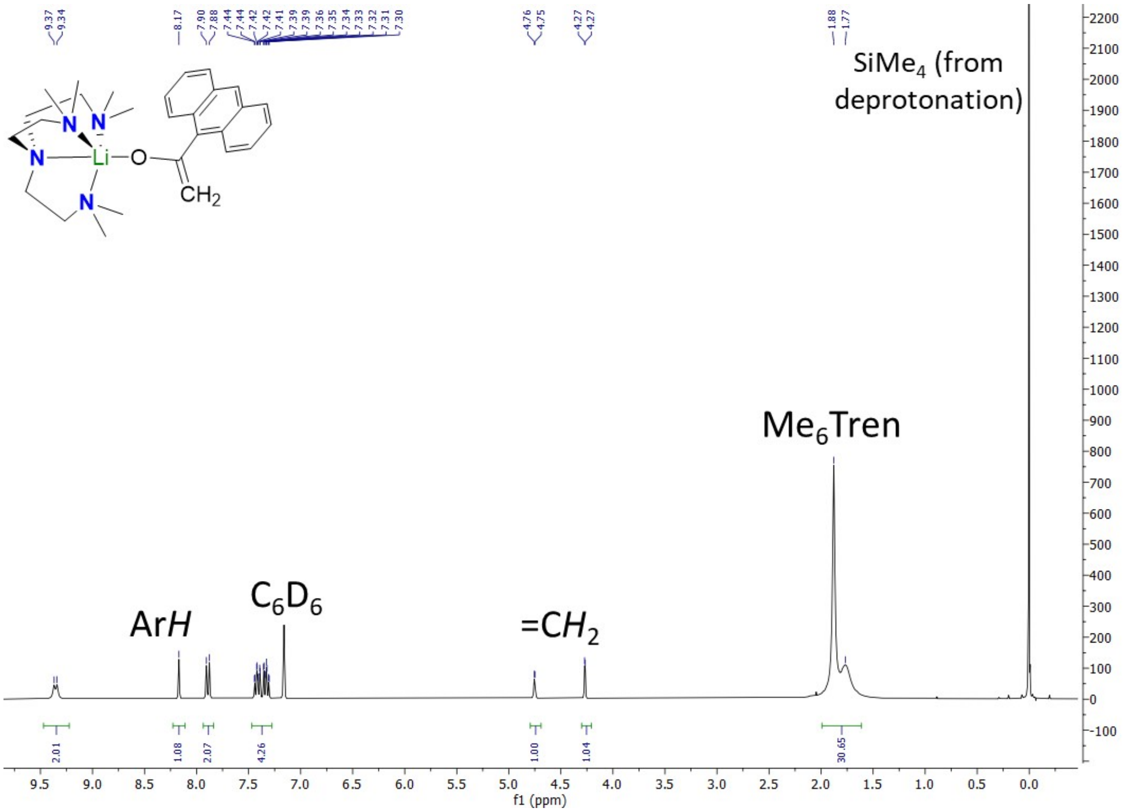

Figure S4: ^{1}H NMR spectrum of an NMR scale reaction between Li(CH_2SiMe_3)(Me_6Tren) and 9-acetylanthracene to form **6-Li** and $SiMe_4$ in C_6D_6 at 298 K.

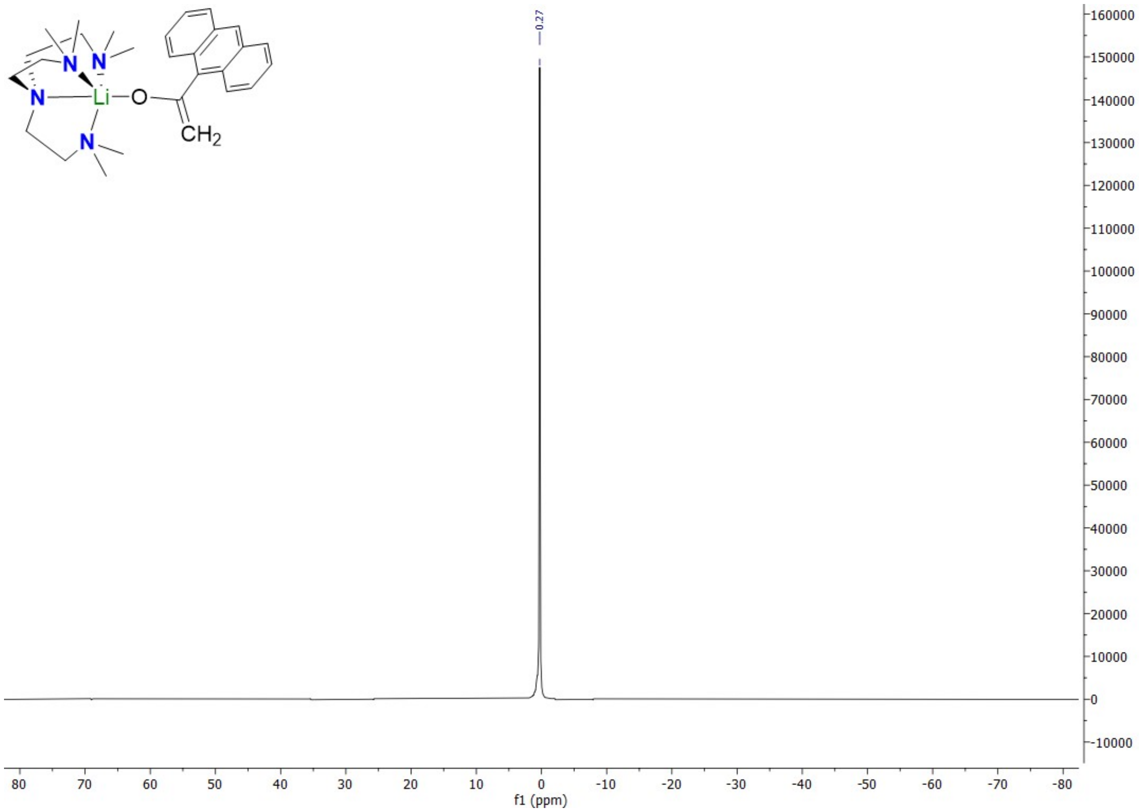

Figure S5: ^{7}Li NMR spectrum of an NMR scale reaction between Li(CH_2SiMe_3)(Me_6Tren) and 9-acetylanthracene to form **6-Li** and $SiMe_4$ in C_6D_6 at 298 K.

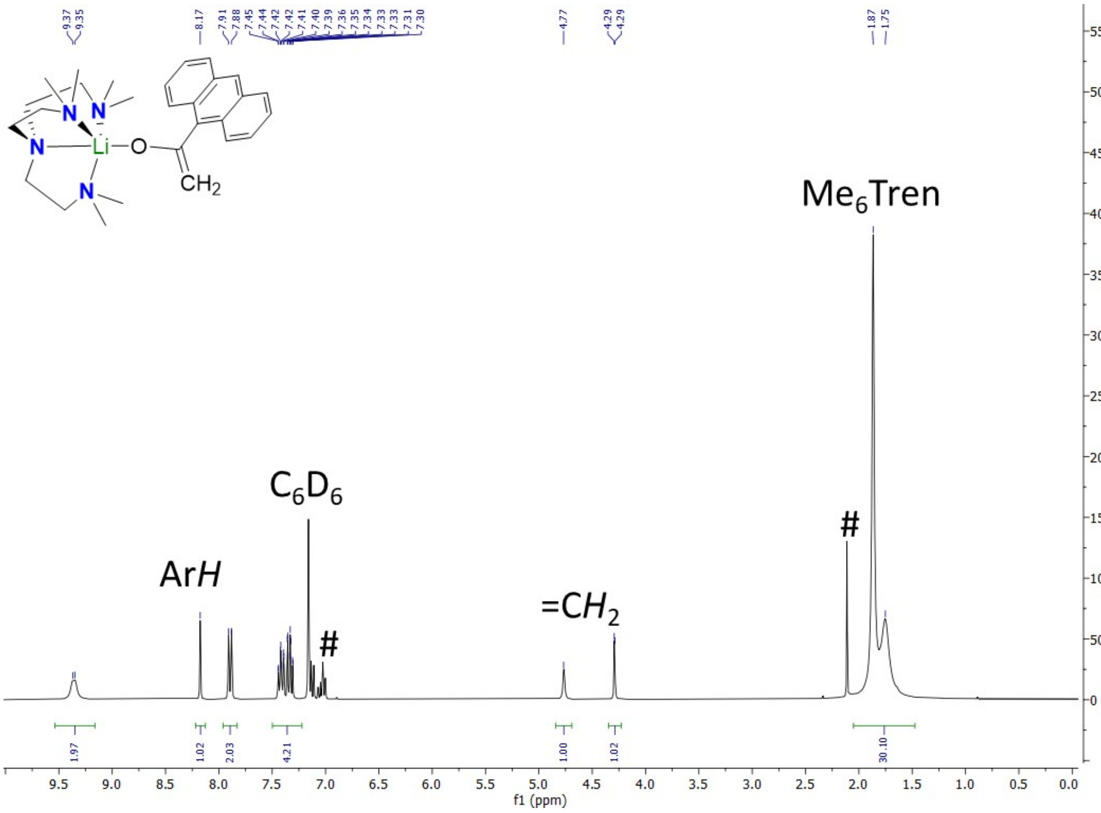

Figure S6: ^{1}H NMR spectrum of isolated **6-Li** in C_6D_6 at 298 K. Signals labelled # = toluene from crystallisation.

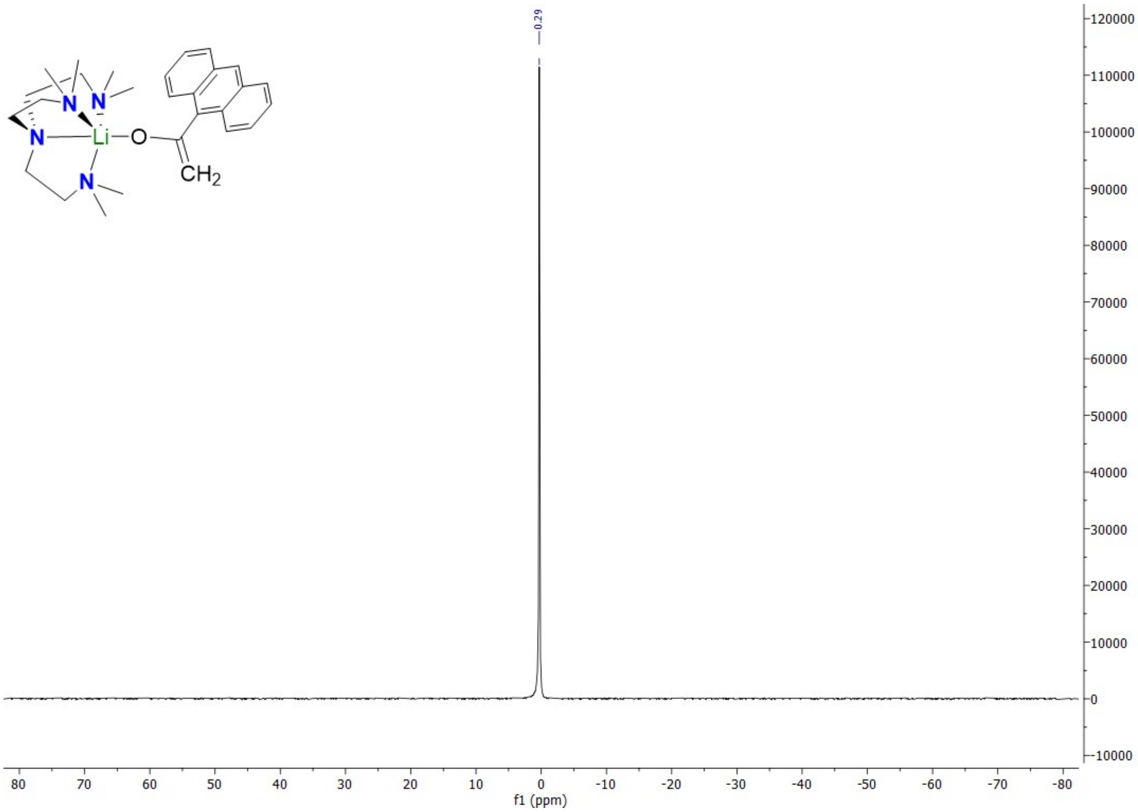

Figure S7: ^{7}Li NMR spectrum of isolated **6-Li** in C_6D_6 at 298 K.

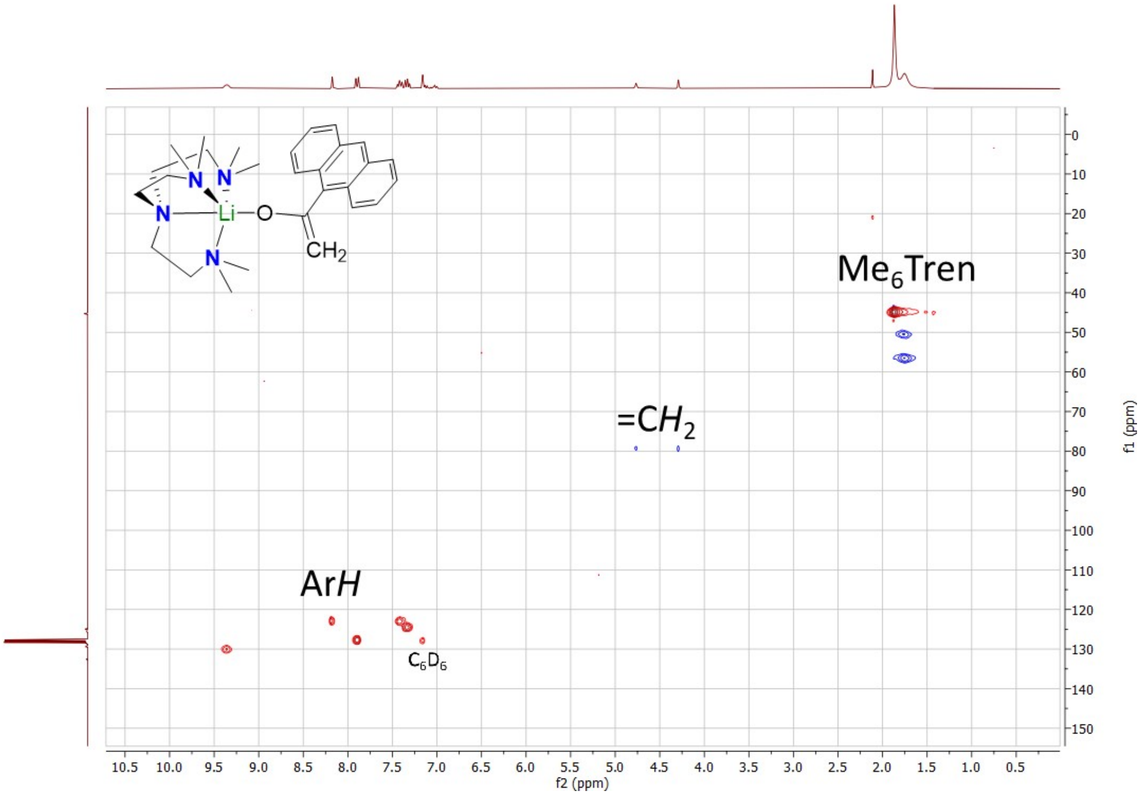

Figure S8: HSQC spectrum of isolated **6-Li**. X-axis = ^{1}H NMR spectrum. Y-axis = ^{13}C NMR spectrum. Red spots = CH or CH$_3$ groups. Blue spots = CH$_2$.

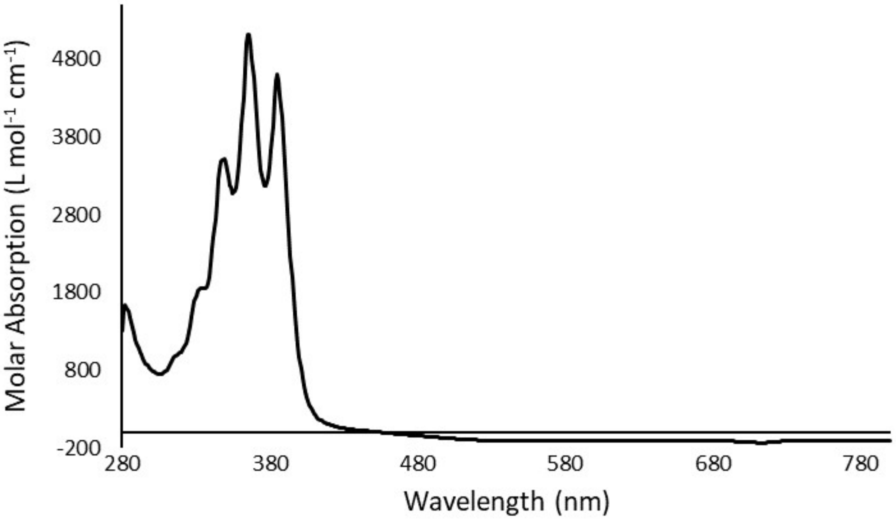

Figure S9: UV/Vis spectrum of **6-Li**. The data was collected on a 0.25 mM benzene solution at 298 K.

Synthesis of 3-Na (NaCH$_2$SiMe$_3$ + 9-acetylanthracene)

NMR scale reaction

9-Acetylanthracene (0.0066 g, 0.03 mmol) was dissolved in C_6D_6 (0.5 ml). The solution was added to $NaCH_2SiMe_3$ (0.0033 g, 0.03 mmol) (almost insoluble in benzene at room temperature) in a one-portion manner. The resulting yellow solution was transferred to a J Young NMR tube. NMR was ran 30 minutes after mixing which showed complete reaction to the enolate. Yellow crystals suitable for SCXRD resulted in the NMR tube.

Scale-up:

9-Acetylanthracene (0.2203 g, 1 mmol) was dissolved in benzene (1 ml). The solution was added to a suspension of $NaCH_2SiMe_3$ (0.1102 g, 1 mmol) in benzene (1 ml), in a one-portion manner and mixed using a pipette. Complete dissolving resulted to form a yellow solution and after 30 seconds a yellow crystalline solid precipitated out. The mixture was left at room temperature for 1 hour before the mother liquor was removed and the resulting pale yellow crystalline solid was dried *in vacuo* (0.1767 g, 73 % yield).

^{1}H NMR (d_6-benzene, 25 ˚C, 300 MHz): δ (ppm) 8.49 – 7.84 (m, 3H), 7.79 – 7.59 (m, br, 2H), 7.30 – 7.01 (m, br, overlapping with C_6D_6, 4H), 4.03 – 3.49 (m, br, 2H).

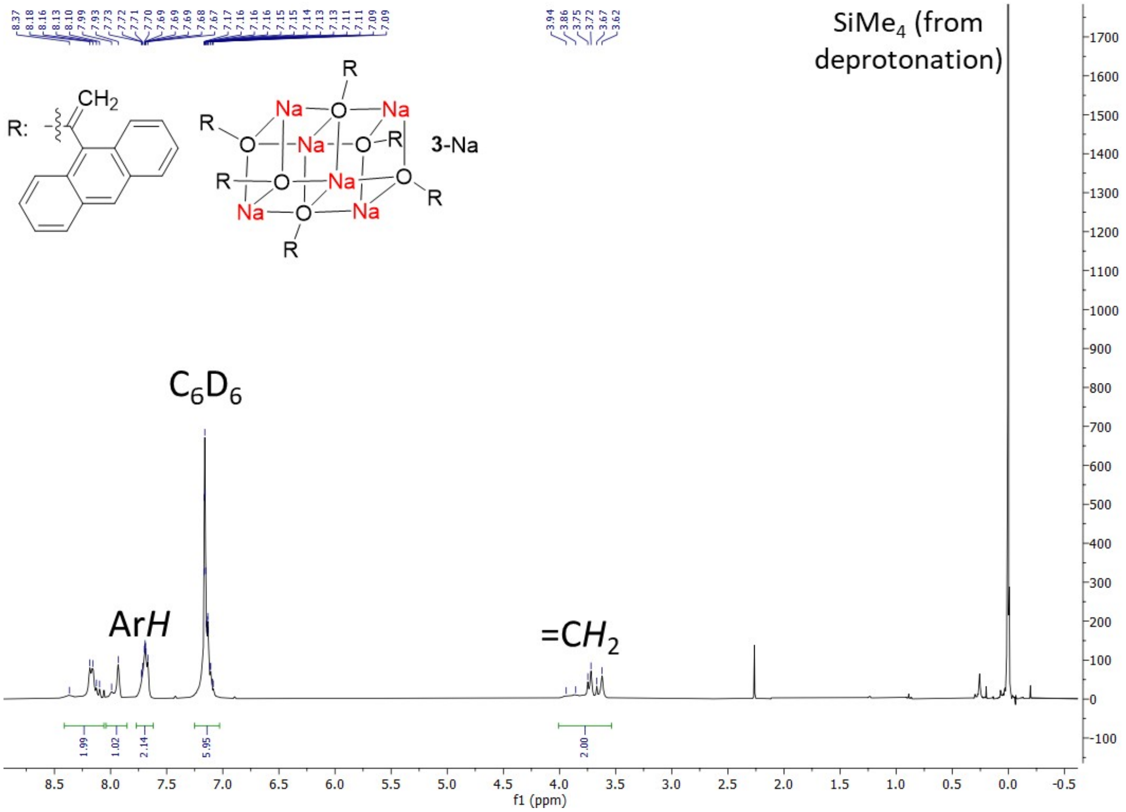

Figure S10: ^{1}H NMR spectrum of an NMR scale reaction between $NaCH_2SiMe_3$ and 9-acetylanthracene to form **3-Na** and $SiMe_4$ in C_6D_6 at 298 K.

Synthesis of 6-Na ([Na(CH_2SiMe_3)(Me_6Tren)] + 9-acetylanthracene)

NMR scale reaction:
[Na(CH$_2$SiMe$_3$)(Me$_6$Tren)] (0.0102 g, 0.03 mmol) was dissolved in C$_6$D$_6$ (0.5 ml). The solution was added to 9-acetylanthracene (0.0066 g, 0.03 mmol) in a one-portion manner. The resulting red solution was transferred to a J Young NMR tube. NMR was ran 30 minutes after mixing which showed complete reaction to the enolate.

Scale-up:
[Na(CH$_2$SiMe$_3$)(Me$_6$Tren)] (0.1703 g, 0.5 mmol) was dissolved in benzene (1 ml). The solution was added to a solution of 9-acetylanthracene (0.1101 g, 0.5 mmol) in benzene (1 ml), in a one-portion manner. The resulting red solution was left at room temperature for 15 minutes, before the volatiles were removed *in vacuo*. A red solid resulted. The solid was dissolved in toluene (2 ml). The resulting solution was filtered and placed in a -35 °C freezer. Red crystals suitable for SCXRD resulted overnight. The mother liquor was removed and the crystals dried *in vacuo* (0.1218 g = 52 % yield).

^{1}H NMR (d$_6$-benzene, 25 ˚C, 300 MHz): δ (ppm) 9.00 (s, br, 2H), 8.07 (s, 1H), 7.81 (d, J = 8.2 Hz, 2H), 7.29 (m, 4H), 4.44 (s, br, 1H), 4.05 (s, br, 1H), 2.06 (m, br, 6H), 1.94 (m, br, 6H), 1.89 (s, 18H).
^{13}C NMR: (d$_6$-benzene, 25 ˚C, 75 MHz): δ (ppm) 132.1 (quaternary Ar*C*), 128.6, 128.0, 124.5 (Ar*C*H), 80.7 (=*C*H$_2$), 80.4 (=*C*H$_2$), 57.2 (Me$_6$Tren-*C*H$_2$), 51.7 (Me$_6$Tren-*C*H$_2$), 45.0 (Me$_6$Tren-*C*H$_3$).

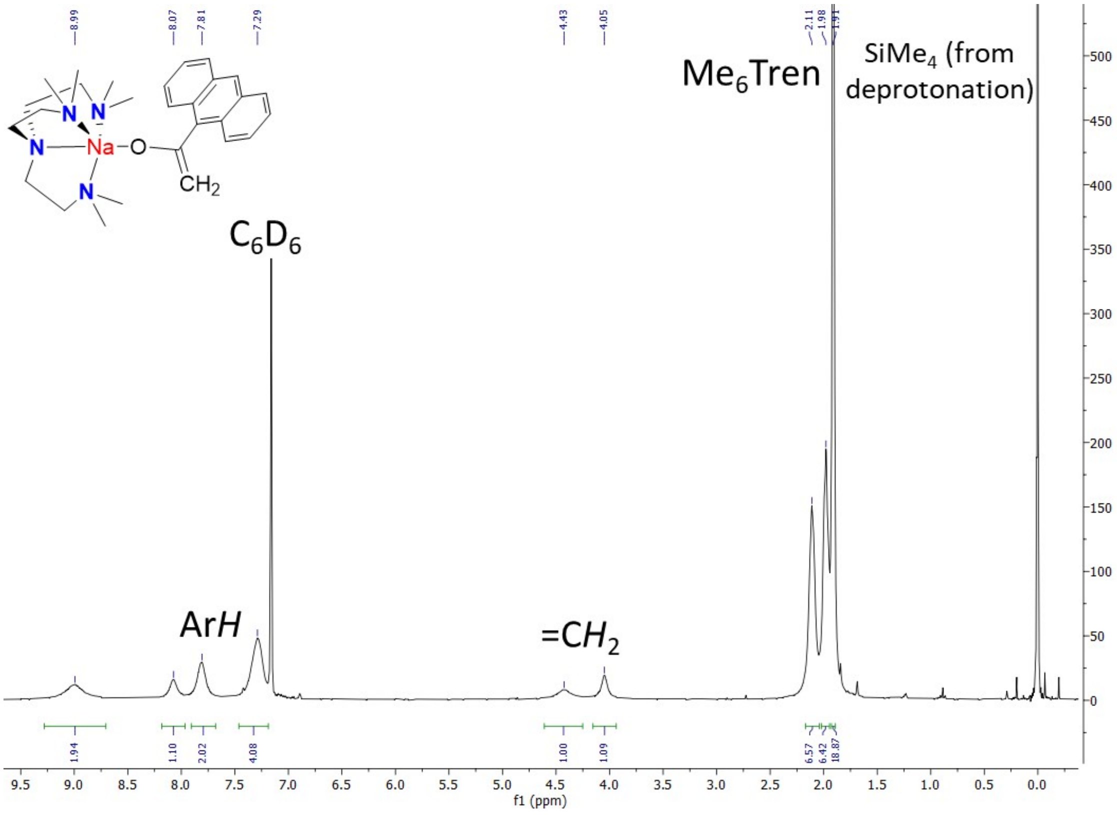

Figure S11: ^{1}H NMR spectrum of an NMR scale reaction between $Na(CH_2SiMe_3)(Me_6Tren)$ and 9-acetylanthracene to form **6-Na** and $SiMe_4$ in C_6D_6 at 298 K.

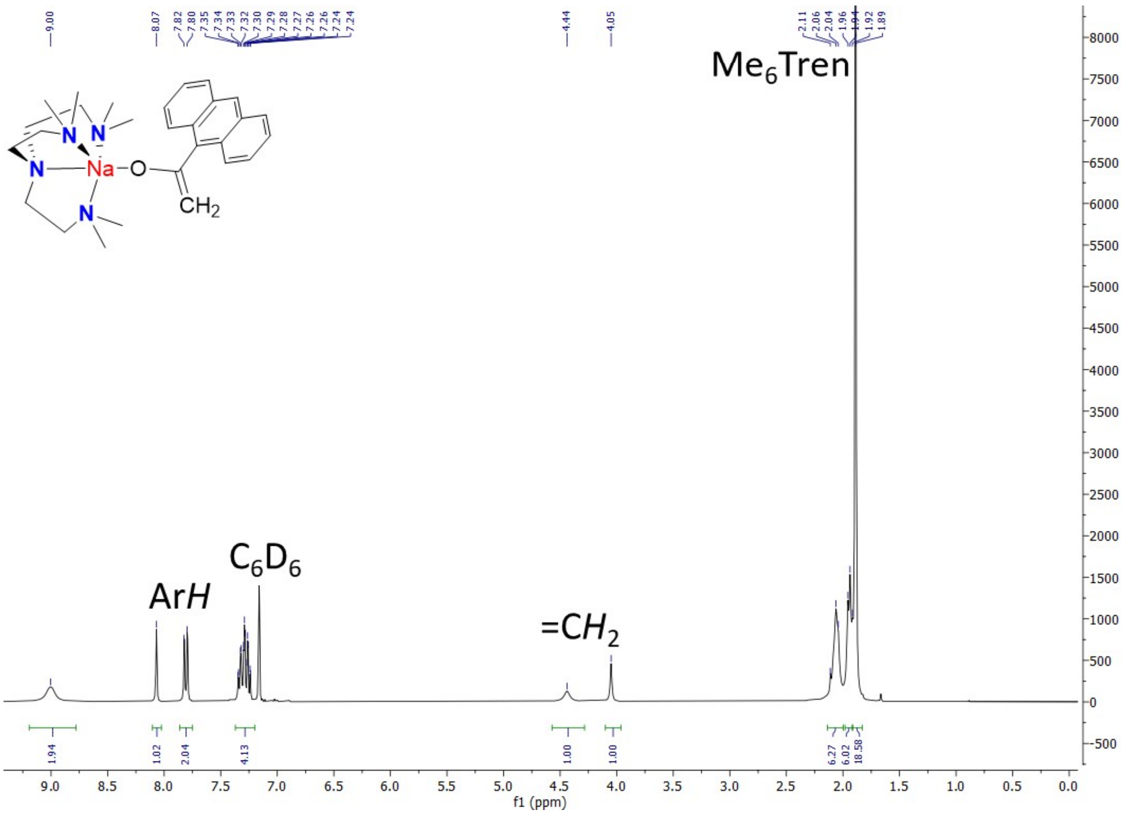

Figure S12: ^{1}H NMR spectrum of isolated **6-Na** in C_6D_6 at 298 K.

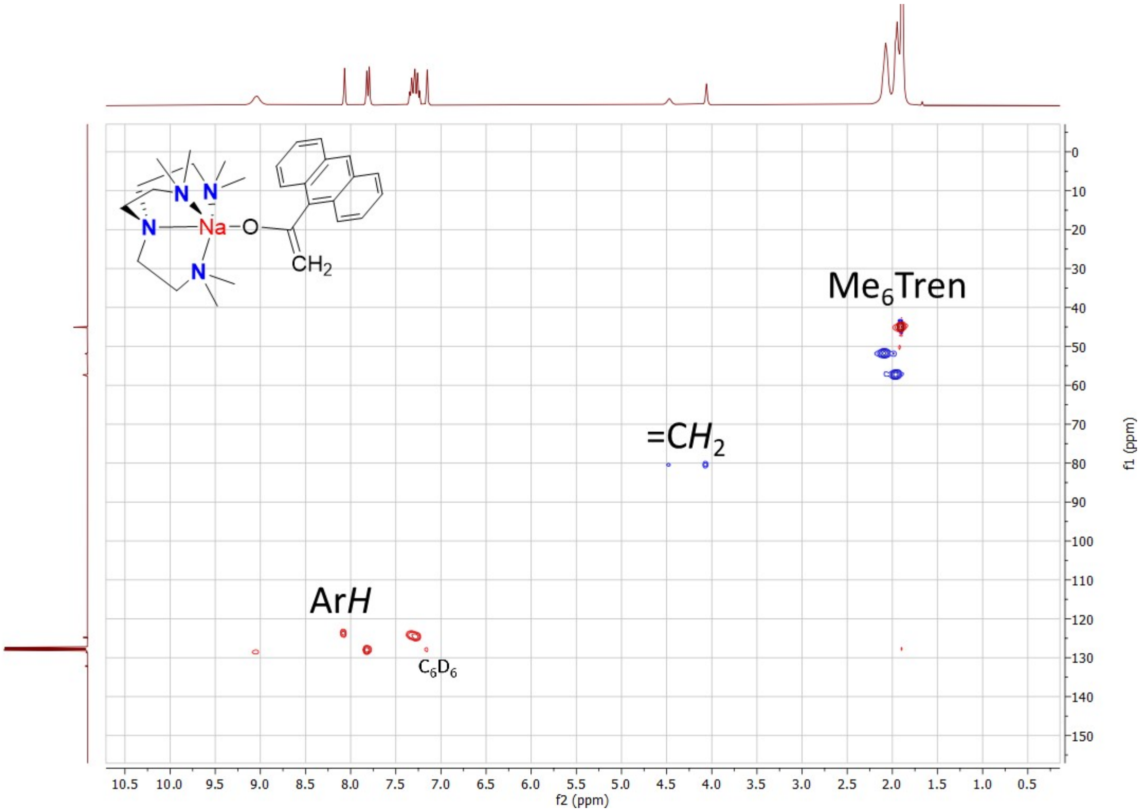

Figure S13: HSQC spectrum of **6-Na**. X-axis = ^{1}H NMR spectrum. Y-axis = ^{13}C NMR spectrum. Red spots = CH or CH$_3$ groups. Blue spots = CH$_2$.

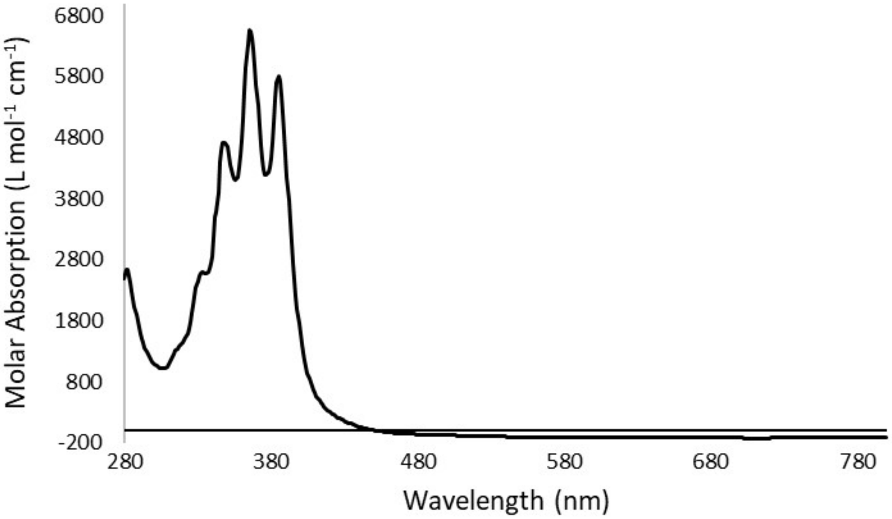

Figure S14: UV/Vis spectrum of **6-Na**. The data was collected on a 0.25 mM benzene solution at 298 K.

Synthesis of 3-K (KCH$_2$SiMe$_3$ + 9-acetylanthracene)

NMR scale reaction

9-Acetylanthracene (0.0066 g, 0.03 mmol) was dissolved in C_6D_6 (0.5 ml). The solution was added to KCH_2SiMe_3 (0.0038 g, 0.03 mmol) in a one-portion manner. The resulting yellow solution was transferred to a J Young NMR tube. NMR was ran 30 minutes after mixing which showed complete reaction to the enolate.

Scale-up:

9-Acetylanthracene (0.1101 g, 0.5 mmol) was dissolved in benzene (2 ml). The solution was added to a KCH_2SiMe_3 (0.1102 g, 1 mmol) in a one-portion manner and mixed using a pipette. Complete dissolving resulted to form a yellow solution and after 1 minute, a yellow crystalline solid precipitated out. The mixture was left at room temperature for 15 minutes before the mother liquor was removed and the resulting pale yellow crystalline solid was dried *in vacuo* (0.1371 g, 86 % yield).

The solid was dissolved in a mixture of toluene (2 ml), benzene (1 ml) and n-hexane (0.5 ml) and the resulting solution was filtered and placed in a -35 °C freezer. Crystals suitable for SCXRD resulted after 4 weeks.

^1H NMR (d_6-benzene, 25 ˚C, 300 MHz): δ (ppm) 8.27 (d, *J* = 8.8 Hz, 2H), 8.19 (s, 1H), 7.91 (d, J = 8.5 Hz, 2H), 7.35 (t, J = 7.5 Hz, 2H), 7.19 – 7.10 (signals overlapping with C_6D_6 signal, m, 2H), 3.77 (s, 1H), 3.68 (s, 1H).

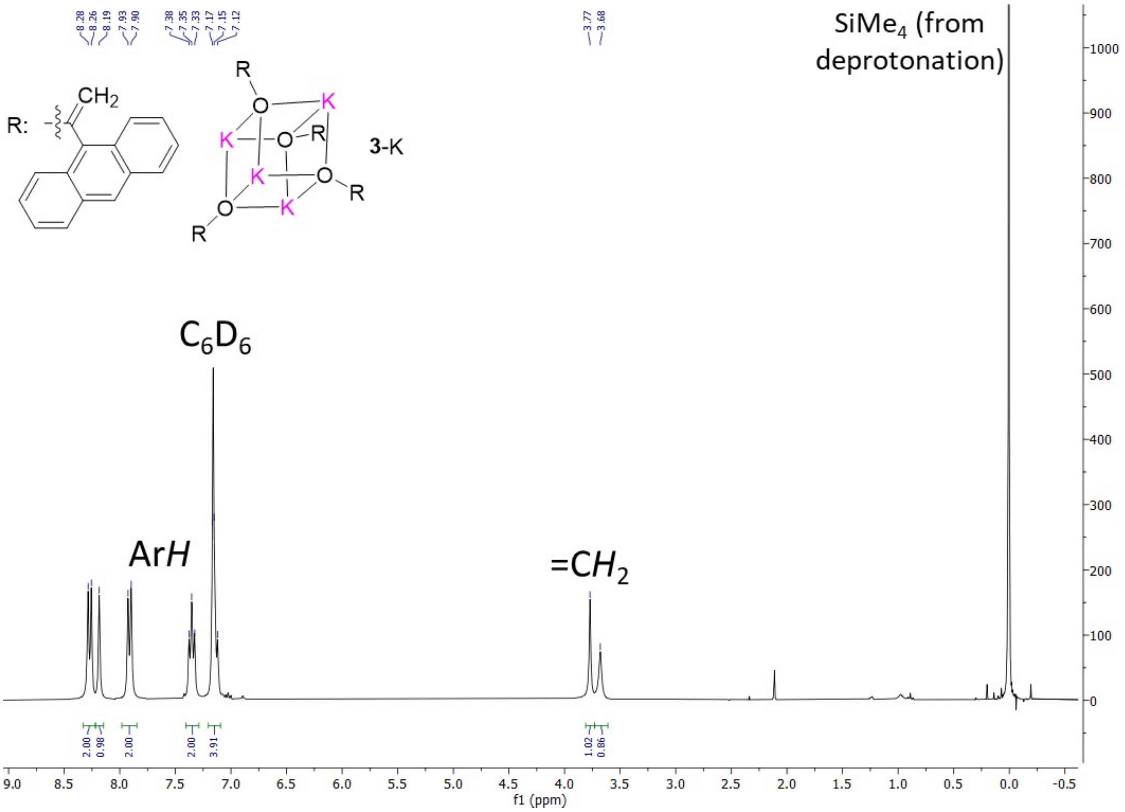

Figure S15: ^1H NMR spectrum of an NMR scale reaction between KCH_2SiMe_3 and 9-acetylanthracene to form **3-K** and $SiMe_4$ in C_6D_6 at 298 K.

Reaction between [K(CH_2Ph)(Me_6Tren)] and 9-acetylanthracene

9-Acetylanthracene (0.0066 g, 0.03 mmol) was dissolved in C_6D_6 (0.5 ml). The solution was added to [K(CH_2Ph)(Me_6Tren)] (0.0108 g, 0.03 mmol) in a one-portion manner. The resulting yellow solution was transferred to a J Young NMR tube. NMR was ran 30 minutes after mixing which showed the same product as in the above reaction and uncoordinated Me_6Tren ligand.

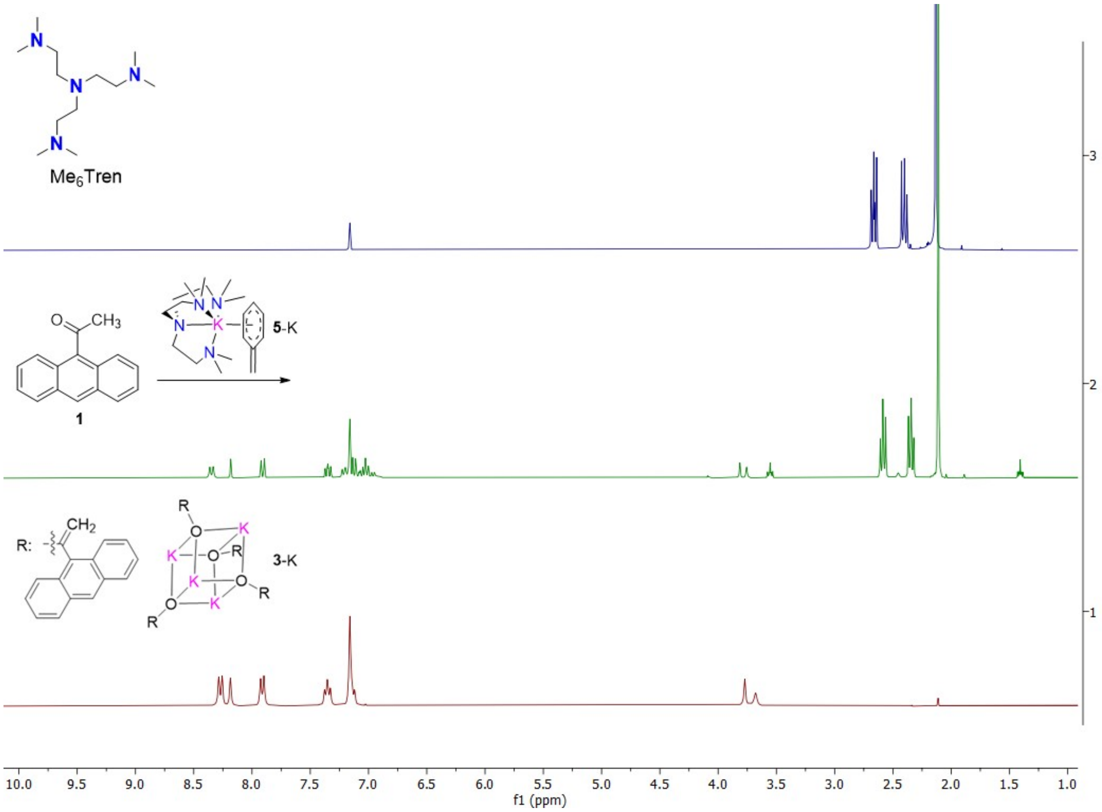

Figure S16: Stacked ^{1}H NMR (C_6D_6, 298 K, 300 MHz) of an NMR scale reaction between **5-K** and 9-acetylanthracene (**1**) (middle: green); authenticated sample of uncoordinated Me$_6$Tren (top: blue); and **3-K** (bottom: red).

3. Single-Crystal X-Ray Crystallographic Data

Table S1. The crystallographic date for 3-Li, 3-Na, 3-K

Complex	**3-Li**	**3-Na**	**3-K**
Empirical formula	$C_{108}H_{78}Li_6O_6$	$C_{22}H_{17}NaO$	$C_{164.9}H_{125.8}K_8O_8$
Formula weight	1513.34	320.35	2548.01
Temperature/K	150.0(2)	150.0(2)	150.0(2)
Crystal system	monoclinic	triclinic	orthorhombic
Space group	Cc	P-1	Pbca
a/Å	19.4816(5)	12.3035(3)	20.2465(4)
b/Å	16.7761(4)	13.3928(3)	24.7118(4)
c/Å	25.2397(6)	17.4184(4)	28.6260(5)
α/°	90	81.860(2)	90
β/°	96.189(2)	85.940(2)	90
γ/°	90	63.004(2)	90
Volume/Å^3	8200.9(3)	2531.60(11)	14322.4(4)
Z	4	6	4
ρ_{calc}g/cm^3	1.226	1.261	1.182
μ/mm^{-1}	0.567	0.814	2.584
F(000)	3168	1008	5325
Crystal size/mm^3	0.1 × 0.08 × 0.05	0.23 × 0.11 × 0.03	0.16 × 0.1 × 0.04
Radiation	CuKα (λ = 1.54184)	CuKα (λ = 1.54184)	CuKα (λ = 1.54184)
2Θ range for data collection/°	6.97 to 156.856	5.126 to 157.434	6.176 to 154.318
Index ranges	-24 ≤ h ≤ 21, -20 ≤ k ≤ 19, -32 ≤ l ≤ 29	-15 ≤ h ≤ 13, -16 ≤ k ≤ 17, -21 ≤ l ≤ 21	-11 ≤ h ≤ 25, -29 ≤ k ≤ 29, -36 ≤ l ≤ 34
Reflections collected	40731	29892	72419
Independent reflections	13627 [R_{int} = 0.0302, R_{sigma} = 0.0294]	10031 [R_{int} = 0.0256, R_{sigma} = 0.0274]	14282 [R_{int} = 0.0269, R_{sigma} = 0.0220]
Data/restraints/parameters	13627/2/1082	10031/0/650	14282/1246/821
Goodness-of-fit on F^2	1.055	1.071	1.039
Final R indexes [I>=2σ (I)]	R_1 = 0.0466, wR_2 = 0.1286	R_1 = 0.0424, wR_2 = 0.1149	R_1 = 0.0555, wR_2 = 0.1630
Final R indexes [all data]	R_1 = 0.0523, wR_2 = 0.1366	R_1 = 0.0508, wR_2 = 0.1204	R_1 = 0.0645, wR_2 = 0.1697
Largest diff. peak/hole / e Å^{-3}	0.37/-0.20	0.51/-0.40	0.49/-0.85

Table S2. The crystallographic date for **6**-Li and **6**-Na

Complex	**6-Li**	**6-Na**

Empirical formula	$C_{63}H_{90}Li_2N_8O_2$	$C_{28}H_{41}N_4NaO$
Formula weight	1005.3	472.64
Temperature/K	150.0(2)	150.0(2)
Crystal system	monoclinic	monoclinic
Space group	$P2_1/n$	$P2_1/c$
a/Å	12.4692(2)	11.3331(5)
b/Å	17.6687(4)	12.8913(5)
c/Å	13.5637(2)	19.8712(9)
α/°	90	90
β/°	95.153(2)	103.504(4)
γ/°	90	90
Volume/Å^3	2976.20(9)	2822.9(2)
Z	2	4
ρ_{calc}g/cm^3	1.122	1.112
μ/mm^{-1}	0.519	0.663
F(000)	1092	1024
Crystal size/mm^3	0.22 × 0.16 × 0.11	0.22 × 0.15 × 0.12
Radiation	CuKα (λ = 1.54184)	CuKα (λ = 1.54184)
2Θ range for data collection/°	8.238 to 156.632	8.024 to 157.564
Index ranges	$-15 \le h \le 11$, $-21 \le k \le 18$, $-17 \le l \le 16$	$-14 \le h \le 14$, $-5 \le k \le 16$, $-25 \le l \le 24$
Reflections collected	23333	19536
Independent reflections	5969 [R_{int} = 0.0275, R_{sigma} = 0.0264]	5608 [R_{int} = 0.0330, R_{sigma} = 0.0323]
Data/restraints/parameters	5969/408/378	5608/0/313
Goodness-of-fit on F^2	1.05	1.043
Final R indexes [I>=2σ (I)]	R_1 = 0.0402, wR_2 = 0.1042	R_1 = 0.0650, wR_2 = 0.1740
Final R indexes [all data]	R_1 = 0.0502, wR_2 = 0.1107	R_1 = 0.0777, wR_2 = 0.1829
Largest diff. peak/hole / e Å^{-3}	0.20/-0.14	0.39/-0.20

Crystal structure data was collected on a XtaLAB Synergy, Single source at home/near, HyPix-Arc 100 diffractometer equipped with an fine-focus sealed X-ray tube ($\lambda_{\text{CuK}\alpha}$ = 1.54184 Å) and an Oxford Cryosystems CryostreamPlus open-flow N_2 cooling device. Cell refinement, data collection and data reduction were undertaken via software

CrysAlisPro 1.171.42.73a (Rigaku OD, 2022). Intensities were corrected for absorption using CrysAlisPro 1.171.42.73a (Rigaku Oxford Diffraction, 2022) Analytical numeric absorption correction using a multifaceted crystal model based on expressions derived by R.C. Clark & J.S. Reid. (Clark, R. C. & Reid, J. S. (1995). Acta Cryst. A51, 887-897) Empirical absorption correction using spherical harmonics, implemented in SCALE3 ABSPACK scaling algorithm.

Using Olex2 (Dolomanov, 2009), the structure was solved using SHELXT 2018/2 (Sheldrick, 2018) and refined by SHELXL 2019/1 (Sheldrick, 2015).

Dolomanov, O.V., Bourhis, L.J., Gildea, R.J, Howard, J.A.K. & Puschmann, H. (2009), J. Appl. Cryst. 42, 339-341.
Sheldrick, G.M. (2008). Acta Cryst. A64, 112-122.
Sheldrick, G.M. (2015). Acta Cryst. A71, 3-8.

Notes on crystallographic data:

3-Na – The structure forms layers of clusters coplanar with the crystallographic (001) plane. The space between layers is occupied by benzene molecules.

3-K – It appears that there are both benzene and toluene molecules occupying the same positions throughout the crystal manifesting as disorder. One such site has been modelled as substitutionally disordered. The occupancy of the methyl group of the toluene was allowed to refine independently of the atomic displacement parameters and fixed before anisotropy was introduced into the model. The asymmetric unit also contains a solvent-accessible void in which there appear to be multiple orientations of both toluene and benzene. An unambiguous model for these solvent molecules in this site could not be achieved and hence the associated electron density was treated using the Olex2 solvent mask routine.

6-Li – The asymmetric unit contains a half a molecule of toluene modelled as disordered over a centre of symmetry. Accordingly, the solvent molecule was modelled in a negative part with an occupancy constrained to be a half. The atomic displacement parameters of all partially- occupied non-hydrogen atoms were restrained using the SIMU card.

4. Computational Details

General

Geometry optimization and vibrational frequency calculations of both **6**-Li and **6**-Na were completed using the hybrid DFT functional B3LYP [6] [7] along with a 6-31+G* basis set for all atoms. The effects of solvent benzene molecules were accounted for through the use of the integral equation formulation of the polarizable continuum model (IEFPCM) as implemented in Gaussian 16. Optimized structures were confirmed to be minima through evaluation of the vibrational frequencies which presented as 3N-6 real numbers for both **6**-Li and **6**-Na. Geometry optimization, vibrational frequency, natural bond orbital analysis [8] and relaxed potential energy surface scan calculations were all completed using the Gaussian 16 package [9]. A comparison between the experimental and optimized bond lengths for both **6**-Li and **6**-Na are shown in Table S3.

Table S3: Experimental and calculated bond lengths of **6**-Li and **6**-Na alongside their percentage change.

	M – O / Å	O – C_a / Å	C_a – C_b / Å	C_a – C_c / Å
6-$Li_{(exp)}$	1.827(2)	1.2836(13)	1.3389(18)	1.5148(14)
6-$Li_{(calc)}$	1.821	1.302	1.366	1.522
%change	*-0.33*	*1.43*	*2.02*	*0.48*
6-$Na_{(exp)}$	2.1324(18)	1.279(3)	1.343(3)	1.521(3)
6-Na $_{(calc)}$	2.143	1.304	1.365	1.520
%change	*0.500*	*1.95*	*1.64*	*-0.07*

References:

---

[1] Davidson, P. J.; Harris, D. H.; Lappert, M. F. *J. Chem. Soc., Dalton Trans.* **1976**, 2268.

[2] (a) Baillie, S. E.; Clegg, W.; García-Álvarez, P.; Hevia, E.; Kennedy, A. R.; Klett, J.; Russo, L. *Chem. Commun.* **2011**, *47*, 388-390; (b) Lynch, J. R.; Kennedy, A. R.; Barker, J.; Reid, J.; Mulvey, R. E. *Helv. Chim. Acta* **2022**, *105*, e202200082; (c) Anderson, D. E.; Tortajada, A.; Hevia, E. *Angew. Chem. Int. Ed.* **2023**, e202218498; (d) Davison, N.; McMullin, C. L.; Zhang, L.; Hu, S. -X.; Waddell, P. G.; Wills, C.; Dixon, C.; Lu, E. *J. Am. Chem. Soc.* **2023**, *145*, 6562-6576.

[3] Clegg, W.; Conway, B.; Kennedy, A. R.; Klett, J.; Mulvey, R. E.; Russo, L. *Eur. J. Inorg. Chem.* **2011**, 721-726.

[4] Davison, N.; Waddell, P. G.; Dixon, C.; Wills, C.; Penfold, T. J.; Lu, E. *Dalton Trans.* **2022**, *51*, 10707-10713.

[5] Davidson, M. G.; Garvia-Vivo, D.; Kennedy, A. R.; Mulvey, R. E.; Robertson, S. D. *Chem. Eur. J.* **2011**, *17*, 3364-3369.

[6] Becke, A. D. *J. Chem. Phys.* **1993**, *98*, 5648.

[7]Lee, C. T.; Yang, W. T.; Parr, R. G. *Phys. Rev. B* **1988**, *37*, 785.

[8] Glendening, E. D.; Reed, A. E.; Carpenter, J. E.; Weinhold, F. NBO Version 3.1, TCI, University of Wisconsin, Madison, 1998.

[9] Gaussian 16, Revision C.01, M. J. Frisch, G. W. Trucks, H. B. Schlegel, G. E. Scuseria, M. A. Robb, J. R. Cheeseman, G. Scalmani, V. Barone, G. A. Petersson, H. Nakatsuji, X. Li, M. Caricato, A. V. Marenich, J. Bloino, B. G. Janesko, R. Gomperts, B. Mennucci, H. P. Hratchian, J. V. Ortiz, A. F. Izmaylov, J. L. Sonnenberg, D. Williams-Young, F. Ding, F. Lipparini, F. Egidi, J. Goings, B. Peng, A. Petrone, T. Henderson, D. Ranasinghe, V. G. Zakrzewski, J. Gao, N. Rega, G. Zheng, W. Liang, M. Hada, M. Ehara, K. Toyota, R. Fukuda, J. Hasegawa, M. Ishida, T. Nakajima, Y. Honda, O. Kitao, H. Nakai, T. Vreven, K. Throssell, J. A. Montgomery, Jr., J. E. Peralta, F. Ogliaro, M. J. Bearpark, J. J. Heyd, E. N. Brothers, K. N. Kudin, V. N. Staroverov, T. A. Keith, R. Kobayashi, J. Normand, K. Raghavachari, A. P. Rendell, J. C. Burant, S. S. Iyengar, J. Tomasi, M. Cossi, J. M. Millam, M. Klene, C. Adamo, R. Cammi, J. W. Ochterski, R. L. Martin, K. Morokuma, O. Farkas, J. B. Foresman, and D. J. Fox, Gaussian, Inc., Wallingford CT, 2016.